A two-step Monte Carlo algorithm for interaction between resonant ions and radio frequency waves

Fundamental Plasma Physics 11 (2024) 100065

Contents lists available at ScienceDirect

Fundamental Plasma Physics

journal homepage: www.elsevier.com/locate/fpp

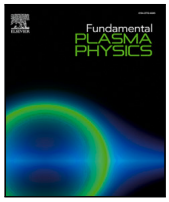

A two-step Monte Carlo algorithm for interaction between resonant ions and radio frequency waves

T. Johnson [a,*], L.-G. Eriksson [b]

[a] Department of Electrical Engineering, KTH Royal Institute of Technology, Stockholm, SE-100 44, Sweden
[b] Department of Space, Earth and Environment,Chalmers University of Technology, Gothenburg, SE-412 96, Sweden

ARTICLE INFO

Keywords:
Fusion
Radio frequency heating
Monte Carlo methods
Wave–particle interactions

ABSTRACT

This paper presents a new Monte Carlo algorithm intended for use in orbit following Monte Carlo codes (OFMC) to describe resonant interaction of ions with Radio Frequency (RF) waves in axi-symmetric toroidal plasmas. The algorithm is based on a quasi-linear description of the wave–particle interaction and its effect on the distribution function of a resonating ion species. The algorithm outlined in the present paper utilises a two-step approach for the evaluation of the Monte Carlo operator that has better efficiency and a stronger convergence than the standard Euler–Maruyama scheme. The algorithm preserves the reciprocity of the diffusion process. Furthermore, it simplifies how the displacement of the resonance position, as a result of wave–particle interaction, is accounted for. Such displacements can have a noticeable effect on the deterministic part of the Monte Carlo operator. The fundamental nature of guiding centre displacements of resonant ions as a result of wave–particle interaction is reviewed.

1. Introduction

Radio Frequency (RF) waves are frequently used in fusion plasmas for auxiliary heating and current drive. For instance, waves in the Ion Cyclotron Range of Frequencies (ICRF) are employed in many present day fusion devices and an ICRF system is planned to be one of the heating systems for ITER. The ICRF wave power is resonantly absorbed by an ion species in the plasma by tuning the wave frequency to its cyclotron motion, but also other ion species than the targeted one can parasitically absorb power if they are resonant with the waves somewhere in the plasma. As a result of absorbing RF wave power, the distribution function(s) of the ion species concerned will be distorted and often non-Maxwellian high energy tails develop. While the study of ion distributions distorted by wave power absorption is of interest in its own right, information on the distribution functions is also critical for integrated modelling of fusion plasma. In particular, the equipartition of collisional power densities to the background species and fusion reaction rates play a crucial role for transport simulations. Furthermore, energetic ions generated by ICRF heating can drive instabilities, and many analyses of such instabilities use calculated distribution functions as input. It is therefore important to develop methods with good physics fidelity to simulate distributions functions in the presence of RF waves.

In present day fusion experiments and, even tough to a lesser extent, in future large devices, the widths of guiding orbits of fast ions interacting with RF-waves cannot normally be neglected. This greatly complicates simulations of ion distribution functions. While the orbit averaged 3D Fokker–Planck equation describing the slowing down of energetic ions, including a full orbit treatment, has been successfully implemented in a code using a finite difference solver [1] and including interaction with RF waves [2], such codes are not available on a routine basis.

An alternative is to use Orbit Following Monte-Carlo (OFMC) codes [3–6], which are simpler to implement and a number of them are on the market. By inclusion of Monte Carlo operators representing wave–particle interaction, such codes can be used for calculating distribution functions of ions interacting with RF waves, see e.g. [4–6]. In order to keep the execution time of OFMCs at manageable levels, accelerated Monte Carlo operators can be employed, see [5] for a detailed discussion. Acceleration of Monte Carlo operators is based on the fact that in high temperature (low collisionality) plasmas, perturbations of ion orbits due to collisions and wave–particle interaction normally are small during one revolution. For this reason, an ion executes many near identical poloidal orbits before it deviates significantly from its initial one. In accelerated Monte Carlo algorithms this fact is used such that during one calculated orbit Monte Carlo operators are applied that represent the accumulated effect of a number of revolutions of the orbit, i.e. one calculated orbit represents a number of revolutions in reality. This effectively reduces the solution of the distribution function

* Corresponding author.
E-mail address: johnso@kth.se (T. Johnson).

https://doi.org/10.1016/j.fpp.2024.100065
Received 20 December 2023; Received in revised form 22 May 2024; Accepted 7 June 2024
Available online 2 July 2024

from 5D to 3D and makes it equivalent to the solution of an orbit averaged Fokker–Planck equation (the only difference is that in an orbit averaged Fokker–Planck equation the integration takes place along an unperturbed orbit whereas in an OFMC with accelerated Monte Carlo operators the integration is along a perturbed orbit). The equivalence between an OFMC solution with accelerated operators and the solution of the orbit averaged Fokker–Planck equation means that the latter can be used to derive the OFMC Monte Carlo operator for RF wave–particle interaction [7].

A package called RFOF [8] based on quasi-linear theory for the wave–particle interaction and using an accelerated Monte Carlo operator has been developed for utilisation in OFMCs, and employed in the ASCOT [9] and SPOT [10] OFMCs. It uses a two-step Monte Carlo algorithm, with convergence properties similar to that of the conventional Euler–Maruyama scheme. The current paper presents a detailed description of a new two-step Monte Carlo algorithm with weak and strong convergence of order 1, i.e. better strong convergence than Euler–Maruyama.

The Monte Carlo operator representing quasi-linear diffusion includes two terms; a random term representing scattering, and a deterministic drift term that is proportional to derivatives of the diffusion coefficient. This drift is critical to ensure the reciprocity of the diffusion process, and an inaccurate evaluation of the drift can drive unphysical inverted populations. However, these derivatives are numerically challenging to perform, see [7]. The algorithm outlined in this paper naturally describes these derivatives in a manner that provides a higher degree of reciprocity for finite Monte Carlo steps, compared to a local evaluation of the diffusion coefficient.

The main difficulty encountered when evaluating the Monte Carlo operator is to account for the displacement of the cyclotron resonance as a result of a resonant interaction. There are two reasons for this displacement: (i) the guiding centre position of a resonant particle evolves during the interaction, and as reviewed in this paper, it can be traced back to absorption of wave momentum, (ii) modification of the Doppler shift, mainly due to a change in parallel velocity during a resonant interaction. In practise, it turns out that the second effect, the displacement due the change of Doppler shift, is the more important one. Neither of these displacements of the resonance position are taken into account in most current implementations of Monte Carlo operators for RF wave–particle interaction, e.g. it is not included in the current version of RFOF [8]. However, it is important to note that it is necessary to account for these displacements to ensure the reciprocity of the quasi-linear diffusion process. Thus, the extra effort needed to include it in an accurate Monte Carlo algorithm is warranted.

Because of the displacement of the resonance position, derivatives with respect to phase space variables imply derivatives also in real space. It is not trivial to find a new resonance point after an update of the velocity space variables, and it is therefore desirable to reduce the number of times quasi-linear diffusion coefficients must be evaluated. In this sense, the two-step algorithm presented here is more efficient than the Euler–Maruyama scheme; the diffusion coefficient only needs to be evaluated at two points with the new algorithm, whereas the standard Euler–Maruyama scheme require three evaluations.

2. Theoretical background

In this section we first review the theory background necessary to formulate the new two-step Monte Carlo operator for RF wave–particle interaction. Then, the basic accelerated Monte Carlo scheme is described.

2.1. The orbit averaged quasi-linear RF operator

An ion interacts resonantly with RF waves when its cyclotron frequency or a harmonic thereof coincides with the Doppler shifted wave frequency, i.e. when $n\omega_c = \omega - \mathbf{k}\cdot\mathbf{v}_g$, where $\mathbf{v}_g$ is the guiding centre velocity and $\mathbf{k}$ is the wave vector. Because of the spatial variation of the magnetic field, this means that for a given wave mode an ion can interact resonantly with it at a finite number of interaction points, i.e. resonances, per revolution of an orbit (up to four for a moderate energy particle on a normal trapped orbit). Consequently, it is logical to apply an OFMC RF Monte Carlo operator at each resonant point such that it changes the velocity and guiding centre position of the particle consistent with the wave–particle interaction at that point.

At this point it is necessary discuss a limitation of the Monte Carlo algorithm presented here, it requires that a spatial map of effective parallel wave numbers is available for each toroidal mode number of the wave (in practise the local resonance is in most cases well approximated by $\omega - k_\parallel v_\parallel - n\omega_{ci} = 0$). Thus, it is not possible to directly use the output from a wave field code that employs a poloidal Fourier decomposition of the wave field. The reason is that it implies a spectrum of parallel wave numbers at each point in space for a given toroidal mode. While one could give Monte Carlo "kicks" for each resonance taking into account the parallel wave number spectrum reconstructed from the toroidal and poloidal modes, it would be very costly numerically. More importantly, the physics would not be correctly described because in reality there should be correlations between the "kicks" caused by neighbouring poloidal mode numbers (note that in contrast to toroidal mode numbers, poloidal mode numbers are not "quantum" numbers since there is no poloidal symmetry in a torus), i.e. the absorption process is non-local in the sense that the change of a energy a particle receives at a point depends on the history of its motion. The complexities of dealing with such non-local effects in the framework of quasi-linear theory have been detailed in Refs. [11,12]. On the other hand, in an orbit following Monte Carlo code one wishes to have a local operator for the wave–particle interaction. The approach adopted in the current paper is to assume that a map of effective parallel wave numbers for each toroidal mode number and point in space is available, such that the dominant effect of the poloidal mode number spectrum is accounted for while maintaining a local operator. This closely follows the procedure often used in wave propagation codes that do not employ Fourier decomposition of the wave field in the poloidal direction. They use an iterative technique where at each step a map of the effective parallel wave number is obtained and used as input for the calculation of dielectric tensor components for the next iteration, see e.g. [13,14]. It should also be remarked that ICRF heating scenarios in tokamaks usually use antenna phasings, such as dipole, that provide spectra peaking at high toroidal mode numbers and aim at strong damping of the waves. For antennas situated in the equatorial plane, the correction to $k_\parallel \approx N_\phi/R$ due to the poloidal modes should then be modest.

As discussed in the introduction, we are interested in an accelerated operator. To this end we define an acceleration factor N_{ACC} such that when the OFMC RF Monte Carlo operator is applied it represents the accumulated effect of N_{ACC} near identical orbit passages of the resonance point (i.e. N_{ACC} revolutions of an ion along its orbit).

Because the orbit averaged Fokker–Planck equation describes the evolution of the distribution function on the time scale of many bounce times, τ_b, i.e. many revolutions of an orbit, an orbit averaged RF wave–particle operator can be used to derive the accelerated OFMC Monte Carlo operator. However, the distribution function in the orbit averaged distribution function is a function of three invariants of the unperturbed motion of a particle and it is therefore necessary to translate from these invariants to the local variables used by an OFMC code (e.g. guiding centre position, parallel velocity and magnetic momentum) to obtain the final form of the operator. A brief description of the relevant steps is given below, where we start by reviewing the quasi-linear operator.

Following [7] we will use a quasi-linear operator derived from the seminal paper by A.N. Kaufman [15], see e.g. [16]. Furthermore, we will assume that the "kicks" a particle receives between successive passages of a resonance are uncorrelated, for discussion of when this assumption is valid see e.g. [17]. We here only state the final form of the orbit averaged quasi-linear operator for a given wave angular frequency, ω toroidal mode number N and cyclotron harmonic interaction number n, for more details of its derivation see Ref. [7]. The operator takes the form,

$$\langle Q(f_0)\rangle = \sum_s g^{-1/2}\frac{\partial}{\partial I^i}\left[g^{1/2}D_s^{ij}\frac{\partial f_0}{\partial I^j}\right], \tag{1}$$

where the subscript s stands for quantities evaluated at a stationary point along a particle orbit, i.e. at a resonance $\omega - \mathbf{k}\cdot\mathbf{v}_g - n\omega_c = 0$, and,

$$D_s^{ij} = D_{0s}n^k n^l \frac{\partial I^i}{\partial J^k}\frac{\partial I^j}{\partial J^l}, \tag{2}$$

$$D_{0s} = \frac{1}{2\tau_b}\left(\frac{Ze}{\omega}\right)^2\left|\int_{t_{s-}}^{t_{s+}} dt\, v_\perp\left[E_+ J_{n-1}\left(\frac{k_\perp v_\perp}{\omega_c}\right) + E_- J_{n+1}\left(\frac{k_\perp v_\perp}{\omega_c}\right)\right]e^{i\phi}\right|^2 \tag{3}$$

and

$$\frac{d\phi}{dt} = \dot{\phi} = \omega - \mathbf{k}\cdot\mathbf{v}_g - n\omega_c. \tag{4}$$

Here, f_0 is the orbit averaged distribution function, and $t_{s+} - t_{s-}$ is the effective time interval during which the contributions to the integral accumulate. In principle we could have labelled $Q(f_0)$, D_s^{ij} and D_{0s} with the triplet ω, N and n, but this makes the notation heavy and we just have to keep in mind that in this paper we always deal with a single triplet. The actions J^i are part of a canonical set of action–angle variables [15], where the associated angles evolve linearly in time with frequencies $\Omega_i = \partial H_0/\partial J^i$, and H_0 is the Hamiltonian of the unperturbed particle motion. Specifically, $J^1 = m\mu/Ze$ is the normalised magnetic moment, where $\mu = mv_\perp^2/2B$ is the magnetic moment, J^2 is the toroidal flux enclosed by the poloidal projection of the particle orbit, $J^3 = p_\phi$ is the canonical toroidal angular momentum, $n^1 = n$ is the cyclotron harmonic of the interaction, and $n^3 = N$ is the toroidal wave number of a wave component. The number n^2 is obtained from the global resonance condition $\omega = \mathbf{n}\cdot\boldsymbol{\Omega}$. For a discussion of this resonance condition and its relation to the local resonance $n\omega_c - \omega + \mathbf{k}\cdot\mathbf{v}_g = 0$, see [16,17]. In particular we have: $\Omega_1 = \langle\omega_c\rangle$ is the orbit averaged cyclotron frequency, $\Omega_2 = 2\pi/\tau_b$ is the bounce frequency, $\Omega_3 = \langle\dot{\phi}\rangle$ the orbit average of $\dot{\phi}$. Furthermore, E_+ is the left hand polarised component of the perpendicular electric field (it rotates in the direction of the ion cyclotron motion), E_- is the right hand component of the electric field, $k_\perp$ is the local perpendicular wave vector, $\mathbf{k}$ is the local wave vector and $\mathbf{v}_g$ is the guiding centre velocity (in practise we will assume that it is dominated by the parallel component). Finally, $\mathbf{I} = \mathbf{I}(\mathbf{J})$, is an arbitrary set of invariants and the Jacobian of the transformation from $\mathbf{J}$ to $\mathbf{I}$ is denoted $\sqrt{g}$.

A particularly simple set of invariants to work with when dealing with cyclotron interactions at a specific toroidal mode, N, and cyclotron harmonic, n, is $\mathbf{I} = (I_\perp, I_\parallel, I_\phi)$ defined as,

$$I_\perp = m\mu\frac{\omega}{nZe}$$
$$I_\parallel = W - I_\perp = \mu B\left(1 - \frac{\omega}{n\omega_c}\right) + \frac{1}{2}mv_\parallel^2$$
$$I_\phi = p_\phi - \frac{N}{\omega}W = \frac{Ze}{2\pi}\psi_p + m\frac{F}{B}v_\parallel - \frac{N}{\omega}\left(\mu B + \frac{1}{2}mv_\parallel^2\right)$$

where W is the kinetic energy of the particle (equal to the Hamiltonian for the unperturbed motion, H_0, when the electrostatic potential is neglected) and $F(\psi) = RB_\phi$. It is straightforward to show that the Jacobian for this set of invariants is given by $\sqrt{g} = m^{-3}/|\partial\mathbf{J}/\partial\mathbf{I}| = n\tau_b/(2\pi\omega)$. Furthermore, using the global resonance condition $\omega = \boldsymbol{\Omega}\cdot\mathbf{n}$ one easily finds for these invariants,

$$n^k\frac{\partial I^i}{\partial J^k} = \omega\delta^{i1}. \tag{5}$$

Consequently, the quasi-linear operator (1) takes the form,

$$\langle Q(f_0)\rangle = \sum_s g^{-1/2}\frac{\partial}{\partial I_\perp}\left[g^{1/2}\omega^2 D_{0s}\frac{\partial f_0}{\partial I_\perp}\right]. \tag{6}$$

This formulation of the quasi-linear operator is equivalent to a random walk where a particle passing a resonance receives a "kick" $\Delta I_\perp$, while $I_\parallel$ and I_ϕ remain unchanged. The variance of this kick is related to the diffusion coefficient, $D_{0s} = \langle(\Delta I_\perp)^2\rangle/2\tau_b$. At this point, we need to explore what a change in $I_\perp$ means for the local phase space variables of a resonant ion, which is important for the subsequent formulation of the Monte Carlo algorithm presented in this paper.

2.2. The impact of $\Delta I_\perp$ on local phase space variables

The purpose of this section is to translate the change in $I_\perp$ into updates of the four local phase space variables. We start by noting that the changes in the energy and the magnetic moment are given by,

$$\Delta W = \Delta I_\perp, \tag{7a}$$
$$\Delta\mu = \frac{nZe}{m\omega}\Delta I_\perp. \tag{7b}$$

As we will show in this subsection, a resonant interaction characterised by $I_\perp \to I_\perp + \Delta I_\perp$ normally give rise to a displacement of the guiding centre position of the resonating ion, i.e. the updated orbit will generally not pass through the original resonance point. The kick $\Delta I_\perp$, along with the conservation of the invariants $I_\parallel$ and I_ϕ, describe the post-interaction orbit. The point along the orbit where the particle should be placed is at the updated resonance position. In order to find this position, we split up the procedure in two parts: first a point on the updated orbit is found; secondly the orbit is followed (by orbit the following code) until the resonance point is encountered. We start by describing a method for finding a point along the orbit, the orbit following to an updated resonance point is discussed in Section 3.4.1 below. The approach we adopt for the first part is to find the shortest step in real space from the encountered resonance position to a point on the updated orbit, i.e. an orbit defined by the invariants $(I_\perp + \Delta I_\perp, I_\parallel, I_\phi)$.

We take a general coordinate system to describe the guiding centre position of a particle $\mathbf{X}_g = (q_1, q_2)$ with metric coefficients g_{ij} and denote the shortest step to an updated orbit with lower case delta, i.e. $\delta\mathbf{X}_g = (\delta q_1, \delta q_2)$. Thus, we seek a point along the post-interaction orbit such that,

$$(\Delta s)^2 = g_{ij}\delta q_i\delta q_j \tag{8}$$

is minimised under the constraint provided by $\Delta I_\parallel = 0$, $\Delta I_\phi = 0$, while $I_\perp$ updated to $I_\perp + \Delta I_\perp$. The constraint is given by

$$G(\Delta I_\perp, \delta q_1, \delta q_2) = \bar{G}_0\Delta I_\perp + \bar{G}_1\delta q_1 + \bar{G}_2\delta q_2 = 0. \tag{9}$$

Using the derivations outlined in Appendix A we may write the change in the parallel velocity as,

$$\Delta v_\parallel = \frac{1}{mv_{\parallel R}}\left[\left(1 - \frac{n\omega_{cR}}{\omega}\right)\Delta W - \mu\frac{\partial B}{\partial q_i}\delta q_i\right] \tag{10}$$

and

$$\bar{G}_0 = \left[\frac{N}{\omega} - \frac{F}{Bv_{\parallel R}}\frac{\omega - n\omega_{cR}}{\omega}\right], \tag{11a}$$
$$\bar{G}_i = -Ze\frac{\partial\psi}{\partial q_i} + \frac{F}{B^2 v_{\parallel R}}\left[\mu B\frac{\partial B}{\partial q_i} + mv_{\parallel R}^2\left(\frac{\partial B}{\partial q_i} - \frac{B}{F}\frac{\partial F}{\partial\psi}\frac{\partial\psi}{\partial q_i}\right)\right],\ i\in\{1,2\}. \tag{11b}$$

Here the subscript R stands for evaluation at the resonance before the update to $I_\perp$.

The shortest step in real space $(\Delta s)^2$, under the constraint (9), can now be found by minimising the Lagrangian,

$$L(\delta q_1, \delta q_2, \lambda) = (\Delta s)^2 + \lambda G \tag{12}$$

with respect to variation of δq_1, δq_2 and the Lagrange multiplier λ. The resulting δq_1 and δq_2 to reach the point on the updated orbit are given by,

$$\delta q_1 = \frac{\left(\bar{G}_2 g_{12} - \bar{G}_1 g_{22}\right)}{\bar{G}_1^2 g_{22} + \bar{G}_2^2 g_{11} - 2\bar{G}_1 \bar{G}_2 g_{12}} \bar{G}_0 \Delta W, \tag{13a}$$

$$\delta q_2 = \frac{\left(\bar{G}_1 g_{12} - \bar{G}_2 g_{11}\right)}{\bar{G}_1^2 g_{22} + \bar{G}_2^2 g_{11} - 2\bar{G}_1 \bar{G}_2 g_{12}} \bar{G}_0 \Delta W. \tag{13b}$$

The physical meaning of these expressions for the change of the guiding centre position during resonant wave–particle interaction may not be immediately obvious, and it is the subject of the next subsection.

An important point to note is that the resonance condition, $\omega - \mathbf{k}\cdot\mathbf{v}_g - n\omega_c = 0$, is in general not fulfilled after the displacement by $\delta\mathbf{X}_g = (\delta q_1, \delta q_1)$. Specifically, $\Delta I_\perp$ implies a deformation of the orbit and change in the guiding centre velocity, thereby changing both the Doppler shift and the cyclotron frequency at the updated resonance position. An accurate formulation of a Monte Carlo algorithm for RF wave–particle interaction must take this fact into account, especially when the electric field varies strongly in space and for particles near tangent resonances (for which the phase integral varies strongly). In this context, it should be remarked that the nowadays popular three ion scheme [18] is indeed characterised by a strong spatial variation of the wave electric field.

2.3. On the physics behind the change of guiding centre during resonant wave–particle interaction

The key factor underpinning the guiding centre shift across flux surfaces during a resonant interaction is the absorption of wave momentum perpendicular to the magnetic field. In order to see this in its most pure form, we consider a low beta tokamak with circular flux surfaces, with $F(\psi) \approx R_0 B_0$, and assume that the parallel velocity is much greater than the drift velocity, i.e. $v_\parallel \gg v_D$ (i.e. we essentially neglect curvature effects during the time of the resonant interaction). As coordinates we use minor radius, r, and normal poloidal angle, θ, such that $g_{11} = 1$, $g_{22} = r^2$ and $g_{12} = 0$. In this case we find approximately,

$$\bar{G}_0 \approx \frac{R\hat{\boldsymbol{\phi}} - \frac{F}{B}\mathbf{b}}{\omega}\cdot\mathbf{k} = R B_\theta \frac{k_\phi B_\theta - k_\theta B_\phi}{\omega B^2} = \frac{k_{\rm dia} R B_\theta}{\omega B}, \tag{14a}$$

$$\bar{G}_1 \approx -Ze\frac{\partial\psi}{\partial r}, \tag{14b}$$

$$\bar{G}_2 \approx 0. \tag{14c}$$

Here $k_{\rm dia}$ is the component of the wave vector in the direction of the ion diamagnetic flow. Inserting these expressions into (13a) yields,

$$\delta r \approx \frac{k_{\rm dia}}{\omega_c \omega}\frac{\Delta W}{m}. \tag{15}$$

This result has been obtained previously, mainly in connection with interaction with short wavelength waves, see e.g. [19,20].

In order to provide an intuitive understanding of the physical origin of this displacement, we start by considering the absorption of a photon with energy, $\hbar\omega$, and momentum in the diamagnetic direction, $\hbar k_{\rm dia}$. The momentum absorbed per unit time corresponds to a force,

$$F_{\rm dia} = \frac{k_{\rm dia}}{\omega}\frac{{\rm d}W}{{\rm d}t}, \tag{16}$$

that is perpendicular to the magnetic field and to $\nabla\psi$ (i.e. $\hat{r}$ in our simple case). It therefore gives rise to an $\vec{F}\times\vec{B}$ drift in the $\nabla\psi$ direction. In our simple case we obtain,

$$\frac{{\rm d}r}{{\rm d}t} = \frac{k_{\rm dia}}{\omega_c\omega}\frac{1}{m}\frac{{\rm d}W}{{\rm d}t}. \tag{17}$$

The discrete version of this is exactly equal to Eq. (15) above. Thus, we conclude that the mechanism behind the shift across flux surfaces of the guiding centre position of a resonating ion is a $\vec{F}\times\vec{B}$ type drift induced by the absorption of wave momentum related to $k_{\rm dia}$. At first it may seem somewhat surprising that this detailed physics is encoded in the evolution of the invariants. However, guiding centre drifts are of course covered by the invariants, and their updates as a result of a resonant interaction therefore take into account the absorbed wave momentum.

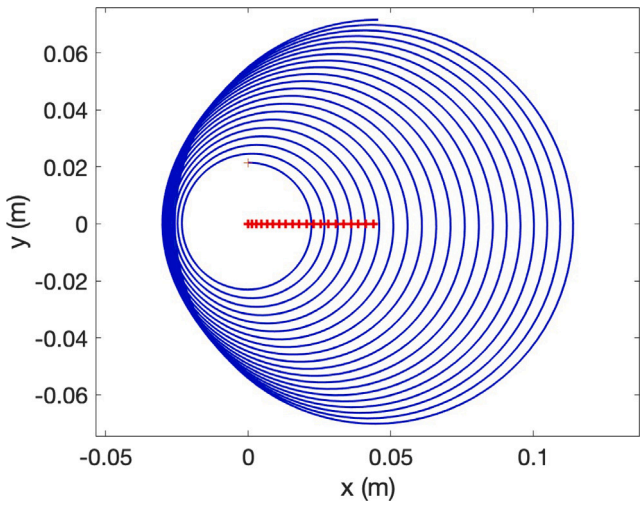

Fig. 1. Evolution of the Larmor orbit for hydrogen ion accelerated from 200 to 2000 keV.

In order to estimate the importance of the displacement of the guiding centre for ICRF accelerated ions, we consider a test case where a hydrogen ion is accelerated continuously from 200 keV to 2 MeV (hydrogen minority ions with 2 MeV energies are typical for high power ICRF heating in a machine like JET), and assume a realistic wave number for ICRF of $k_{\rm dia} = 20\,{\rm m}^{-1}$ and a magnetic field of 3 T. For simplicity we have integrated the motion of a resonating ion in a straight magnetic field to study the displacement of the guiding centre. We have assumed that the electromagnetic field is proportional to $\exp[i(\omega t - k_{\rm dia} y)]$ and that the electric field is purely left hand polarised (i.e. turning in the same direction as the ion in the simulation). The resulting evolution of the orbit is shown in Fig. 1. The guiding centre is estimated each time the particle passes $y = 0$ on the right-hand side, and marked with red "+" signs in Fig. 1. A comparison between the simulated guiding centre position and the one obtained from Eq. (15) is shown in Fig. 2. In reality, of course, the acceleration during ICRF interaction takes place during a large number of consecutive crossings of a resonance, and the results shown in Figs. 1 and 2 are just to illustrate the mechanism behind the displacement of the guiding centre of a resonating ions in its pure form. They also provide a rough estimate of the importance of the effect.

As can be seen, the agreement between the simulated guiding centre position and that from Eq. (15) is very good. We can see that the guiding centre position is displaced by about 5 cm in the simulated case. While this is not a very strong effect, it is still sufficiently significant that it should be accounted for in detailed simulations of high power ICRF heating in tokamaks.

3. Monte Carlo algorithms for RF wave–particle interaction

The principle behind the Monte Carlo technique is to follow a large number of Monte Carlo "particles" or "markers" whose positions in phase space are periodically updated by the application of Monte Carlo operators representing various processes (collisions, wave–particle interaction etc.). In order to find practical Monte Carlo algorithm describing wave–particle interaction for implementation in an OFMC we first need to study the Langevin equation and the associated Itô integral. Discretisation of the latter is the key step in developing

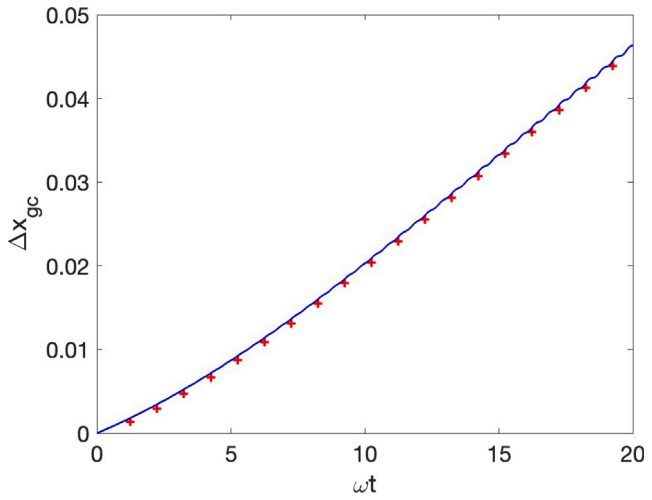

Fig. 2. The simulated evolution of guiding centre position is shown in the solid blue curve, and the evolution described in Eq. (15) is shown as the red crosses.

the Monte Carlo operators, and below the standard Euler–Maruyama scheme will be reviewed before the new improved two-step scheme is introduced.

3.1. The Langevin equation and the Itô integral

We start by assuming that at a point in time $t = t_0$ a Monte Carlo marker is located at $\mathbf{I} = \mathbf{I}_0$. The orbit averaged distribution function for this single Monte Carlo particle can formally be written as: $f_0^1(t_0, \mathbf{I}) = g^{-1/2}\delta(\mathbf{I} - \mathbf{I}_0)$. In order to calculate the evolution of the marker position in phase space during a time $t - t_0$ we turn to the Langevin equation, a stochastic differential equation, corresponding to the quasi-linear operator. In order for the stochastic equation to be equivalent to the quasi-linear operator, the time evolution of the expectation value, $\langle I^i \rangle$, and the variance, $\sigma^{ij} = \langle (I^i - \langle I^i \rangle)(I^j - \langle I^j \rangle) \rangle$, for an initial one-particle distribution must be identical. Starting from the one-particle distribution function, one obtains these two quantities by taking moments of the quasi-linear operator. With our chosen invariants, only $I_\perp$ evolves during the resonant interaction and one simply finds,

$$\frac{d\langle I_\perp \rangle}{dt} = \frac{1}{\tau_b}\frac{\partial}{\partial I_\perp}[\tau_b \omega^2 D_{0s}],$$
$$\frac{d\langle I_\parallel \rangle}{dt} = 0,$$
$$\frac{d\langle I_\phi \rangle}{dt} = 0,$$
$$\frac{d\sigma^{ij}}{dt} = 2\omega^2 D_{0s}\delta^{i,1}\delta^{j,1}.$$

Next, we introduce a normalised time $\tau = t/\tau_b$ and a normalised diffusion coefficient $\bar{D}_{0s}$

$$\bar{D}_{0s} = \tau_b \omega^2 D_{0s}. \tag{18}$$

Note that, according to Eq. (3), $\bar{D}_{0s}$ is independent of τ_b. This enables us to construct a local operator that does not depend on the bounce time or other global quantities.

The coefficients of the Langevin equation related to $I_\perp$ can then be written in terms of either $\bar{D}_{0s}$, or $\bar{b}_{0s} = \sqrt{2\bar{D}_{0s}}$, as

$$\frac{d\langle I_\perp \rangle}{d\tau} = \frac{\partial \bar{D}_{0s}}{\partial I_\perp} = \bar{b}_{0s}\frac{\partial \bar{b}_{0s}}{\partial I_\perp},$$
$$\frac{d\sigma^{ij}}{d\tau} = 2\bar{D}_{0s}\delta^{i,1}\delta^{j,1} = \bar{b}_{0s}^2\delta^{i,1}\delta^{j,1}.$$

The time evolution of $I_\perp$ for a marker particle having $I_\perp(t_0) = I_{\perp 0}$ with probability one, can be written in the form of an Itô integral as,

$$I_\perp(\tau) = I_{\perp 0} + \int_{\tau_0}^{\tau} \bar{b}_{0s}(I_\perp(\tau'), I_\parallel, I_\phi)\frac{\partial \bar{b}_{0s}(I_\perp(\tau'), I_\parallel, I_\phi)}{\partial I_\perp}\,\mathrm{d}\tau' + \int_{\tau_0}^{\tau} \bar{b}_{0s}(I_\perp(\tau'), I_\parallel, I_\phi)\,\mathrm{d}W_{\tau'}$$

where W_τ is a Wiener process. Here the integration interval, from 0 to τ, may cover a large number of real poloidal revolutions of an orbit. In order to obtain a practical implementation of the above Itô integral for an OFMC we need to develop a discrete version of it. In the next subsections we first outline the standard Euler–Maruyama discretisation and then the new two-step method.

3.2. Euler–Maruyama discretisation

The standard Euler–Maruyama discretisation of the Itô integral on a time grid $\tau_{n+1} = \tau_n + \Delta\tau$ reads,

$$I_\perp(\tau) = I_{\perp 0} + \sum_n \bar{b}_{0s,n}\frac{\partial \bar{b}_{0s,n}}{\partial I_\perp}\Delta\tau_n + \bar{b}_{0s,n}W_{\Delta\tau_n}, \tag{19}$$

where $\bar{b}_{0s,n} = \bar{b}_{0s}\left(I_\perp(\tau_n), I_\parallel, I_\phi\right)$.

We now concentrate on a single time step in the sum above. Because we are using the orbit averaged operator, the normalised time step $\Delta\tau$ corresponds to the number of successive passages of the resonance, i.e. the acceleration factor, $\Delta\tau = N_{ACC}$. Consequently, we obtain for a single step of the Euler–Maruyama scheme,

$$\Delta I_\perp = I_\perp(\tau_{n+1}) - I_\perp(\tau_n) = \bar{b}_{0s,n}\frac{\partial \bar{b}_{0s}}{\partial I_\perp}\bigg|_{\tau=\tau_n} N_{ACC} + \bar{b}_{0s,n}\sqrt{N_{ACC}}W_1, \tag{20}$$

where the Wiener process has been re-scaled, $W_{\Delta\tau} \to \sqrt{N_{ACC}}W_1$.

A difficulty in evaluating the operator above is that it involves taking the partial derivative of $\bar{b}_{0s}$ with respect to $I_\perp$. A numerical evaluation of $\partial\bar{b}_{0s}/\partial I_\perp$ necessitates taking a fictitious step $\delta I_\perp$ and evaluate $\bar{b}_{0s}$ at $I_\perp - \delta I_\perp$ and $I_\perp + \delta I_\perp$. This is somewhat involved because, as already discussed, the modified $I_\perp$ corresponds to a new orbit with a new resonance position and a new phase integral. For this reason, one would like to reduce the number of extra points where $\bar{b}_{0s,n}$ has to be evaluated.

3.3. The new two-step Monte Carlo scheme

As an alternative to the Euler–Maruyama scheme, a two-step predictor–corrector scheme was suggested by Steinbrecher [21] and a basic version was implemented in the RFOF package reported in [8]. This schemes has similar convergence properties to the Euler–Maruyama scheme, but requires only two evaluations of $\bar{b}_{0s}$, one at the initial point and one at the predictor point. Here we propose a new improved two-step scheme designed to achieve a fast strong convergence without adding additional evaluations of $\bar{b}_{0s}$. In this scheme the predictor-step is given by,

$$\delta I_\perp^P(t_n) = \bar{b}_{0s,n}\sqrt{N_{ACC}}W_1. \tag{21}$$

The corrector-step, i.e. the actual update of the marker position in phase space, is then given by,

$$\Delta I_\perp = \frac{1}{2}\bar{b}_{0s,n}\frac{\bar{b}_{0s,n}^P - \bar{b}_{0s,n}}{\delta I_\perp^P}N_{ACC} + \frac{1}{2}\left(\bar{b}_{0s,n}^P + \bar{b}_{0s,n}\right)\sqrt{N_{ACC}}W_1, \tag{22}$$

where $\bar{b}_{0s,n}^P = \bar{b}_{0s}\left(I_\perp(\tau_n) + \delta I_\perp^P(\tau_n), I_\parallel, I_\phi\right)$. Note that the predictor–corrector two-step scheme involves evaluating $\bar{b}_{0s}$ in only two points, while the Euler–Maruyama scheme, with a numerical derivative, require computation of $\bar{b}_{0s}$ in three points.

As shown in Appendix B this two-step scheme has both weak and strong convergence of order 1, which is equivalent of a Milstein scheme [22]. Consequently, the two-step scheme is able to accurately

reproduce the reciprocity of the diffusion process. Specifically, if a Wiener process, sampled as W_s, generates a transition from a state A to a state B, then taking a second step with the value of the Wiener process select to be $-W_s$ generates a transition from B to A', such that $A - A' \sim N_{ACC}^{3/2}$.

The two-step scheme presented above can become numerically inaccurate if the predictor step $\delta I_\perp^P(t_n)$ is so small that significant truncation errors appear in the ratio $\left(\bar{b}_{0s,n}^P - \bar{b}_{0s,n}\right)/\delta I_\perp^P$. This can be resolved by evaluating the ratio using an enlarged version of the predictor step, $\delta I_\perp^{P,enl}$, chosen such that $\bar{b}_{0s,n}$ changes significantly, but still approximately linearly, in the interval from $I_\perp(t_n)$ to $I_\perp(t_n)+\delta I_\perp^{P,enl}$. The corrector step can then be written as,

$$\begin{aligned}\Delta I_\perp = &\frac{1}{2}\bar{b}_{0s,n}\frac{\bar{b}_{0s,n}^{P,enl} - \bar{b}_{0s,n}}{\delta I_\perp^{P,enl}} N_{ACC} \\ &+ \frac{1}{2}\left(\bar{b}_{0s,n}^{P,enl}\frac{\delta I_\perp^P}{\delta I_\perp^{P,enl}} + \bar{b}_{0s,n}\right)\sqrt{N_{ACC}} W_1,\end{aligned} \tag{23}$$

where the diffusion coefficient after the enlarged predictor step is given by

$$\bar{b}_{0s,n}^{P,enl} = \bar{b}_{0s,n}\left(I_\perp(t_n) + \delta I_\perp^{P,enl}, I_\parallel, I_\phi\right). \tag{24}$$

3.4. Practical considerations concerning the new two-step Monte Carlo scheme

Before we enter into a discussion of technical details concerning the implementation of the two-step scheme described in the previous section, it is first worth considering if the displacement of the resonance point after $\delta I_\perp^P$ is significant for a typical case. We concentrate on the effect that turns out to be the most important, namely the change of the Doppler shift. First we note that the toroidal mode number spectrum most frequently used in ICRF heating scenarios peaks at high toroidal mode numbers, such that $k_\parallel \approx N/R$. We also assume $B \approx B_0 R_0/R$. From the resonance condition we then find that a kick in the parallel velocity leads to a displacement in the major radius at the resonance point given by $\Delta R = (N/\omega)\Delta v_\parallel$. Furthermore, the kick in parallel velocity during wave–particle interaction can be related to energy kick as $\Delta v_\parallel = k_\parallel/(m\omega)\Delta W$ (a relation that can be found be considering the absorption of a wave quanta, $\Delta W = \hbar\omega$ and $m\Delta v_\parallel = \hbar k_\parallel$). Thus, the resulting change in major radius at the resonance point is given by $\Delta R = (N/\omega)^2 v\Delta v/R$. Consider now a 1 MeV hydrogen ion in a JET size plasma, with $N = 30$ (typical for dipole phasing of JET antennas), and take a velocity kick of $\Delta v/v = 10\%$. The displacement is then $\Delta R \approx 6$ cm, which is significant, especially for cases like the three ion scheme where E_+ can vary significantly over such distances. Consequently, the real space displacement of the resonance position can play an important role for the expectation value of the Monte Carlo operator in Eq. (22)

Application of the two-step Monte Carlo scheme presented in the previous subsection is fairly straightforward. Nevertheless, in the light of the example above, a complication arises because of the need to evaluate $\bar{b}_{0s,n}^P$ at the resonance point along the orbit corresponding to the predictor, $I_\perp+\delta I_\perp^P$. As discussed in Section 2.2, a point on this orbit can easily be found by calculating $(\delta q_1(\delta I_\perp^P), \delta q_2(\delta I_\perp^P))$ from Eqs. (13a), (13b), but this point will generally not coincide with the modified resonance point along the orbit. It is therefore necessary to explore the orbit around this position to find the resonance location where $\bar{b}_{0s,n}^P$ should be evaluated. In the next subsection an algorithm for finding the new resonance position is outlined and in the subsequent section the complete two-step Monte Carlo algorithm is described.

3.4.1. Finding the resonance point for the orbit corresponding to the predictor $I_\perp + \delta I_\perp^P$

In the previous section a single point on the updated orbit has been found. However, as already discussed this point does in general not coincide with the cyclotron resonance position. Here we present an algorithm, using the OFMC solver, to determine the new resonance position.

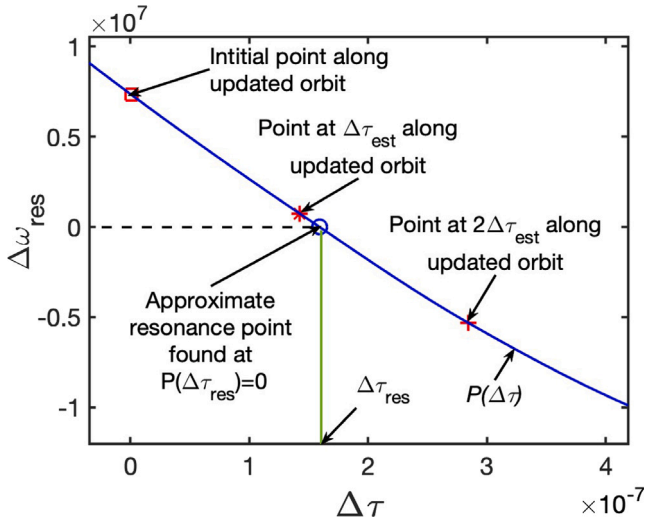

Fig. 3. Illustration of procedure to determine $\Delta\tau_{res}$ for the updated orbit $I_\perp \to I_\perp+\delta I_\perp^P$.

The goal is to find a point along the orbit where the frequency mismatch,

$$\Delta\omega_{res}(\mathbf{X}_g) = \omega - \mathbf{k}(\mathbf{X}_g)\cdot\mathbf{v}_g(\mathbf{X}_g) - n\omega_c(\mathbf{X}_g),$$

is approximately equal to zero. Here $\mathbf{X}_g(t) = (q_1(t), q_2(t))$. We also denote the initial point on the new orbit $\mathbf{X}_{g,0} = (q_1(t_n)+\delta q_1, q_2(t_n)+\delta q_2)$, where t_n is the time at which the particle reaches the resonance.

To lowest order, the time step to reach the resonance, $\Delta\omega_{res} = 0$, is given by

$$\begin{aligned}\Delta\tau_{est} &= \frac{\Delta\omega_{res}(\mathbf{X}_{g,0})}{\frac{d}{d\tau}\left(\mathbf{k}\cdot\mathbf{v}_g + n\omega_c\right)} \\ &\approx \frac{\Delta\omega_{res}(\mathbf{X}_{g,0})}{\Delta\omega_{res}(\mathbf{X}_g(t_{n-1})) - \Delta\omega_{res}(\mathbf{X}_g(t_{n-2}))}\left(t_{n-1} - t_{n-2}\right)\end{aligned}$$

where $\mathbf{X}_g(t_{n-1})$ and $\mathbf{X}_g(t_{n-2})$ are the positions of the two previous time steps of the OFMC, before reaching the resonance.

We are now ready to use the OFMC to take a step $\mathbf{X}_{g,0} \to \mathbf{X}_{g,\Delta\tau_{est}} \equiv \mathbf{X}_{g,0} + \int^{\Delta\tau_{est}} \dot{\mathbf{X}}_g\big|_{OFMC} d\tau$. An improved estimate of time needed to reach the resonance position can now be found as,

$$\Delta\tau_{res} \approx \Delta\tau_{est}\frac{\Delta\omega_{res}(\mathbf{X}_{g,0})}{\Delta\omega_{res}(\mathbf{X}_{g,0}) - \Delta\omega_{res}(\mathbf{X}_{g,\Delta\tau_{est}})}. \tag{25}$$

At this point the final resonance position can be calculated by integrating the orbit with the OFMC, $\mathbf{X}_{g,0} \to \mathbf{X}_{g,\Delta\tau_{res}}$, which is the point where $\bar{b}_{0s,n}^P$ should be evaluated.

In some cases, especially for resonances near the banana tip of a trapped particle, it may be necessary to locate the resonance point with better accuracy, and/or determine the second derivative of $\mathbf{k}\cdot\mathbf{v}_g+n\omega_c$. In this case one can first advance along the orbit a time step $\Delta\tau_{est}$ and then take a second step with the same $\Delta\tau_{est}$. This provides three values of the frequency mismatch at three locations : $\Delta\omega_{res}(\mathbf{X}_{g,0})$, $\Delta\omega_{res}(\mathbf{X}_{g,\Delta\tau_{est}})$ and $\Delta\omega_{res}(\mathbf{X}_{g,2\Delta\tau_{est}})$. One can then fit a second order polynomial, $P(\Delta\tau)$, to these points. To a good approximation the time step required to reach the resonance is then obtained from $P(\Delta\tau_{res}) = 0$. This procedure is illustrated in Fig. 3.

3.4.2. Sketch of the implementation of the new two-step Monte Carlo algorithm

The procedure to evaluate the two-step Monte Carlo operator can be summarised as follows:

1. When a resonance with a wave component with toroidal mode number N is detected, first calculate the predictor step $\delta I_\perp^P$, which implies a modified orbit.
2. Move to a point on the modified orbit, i.e. $\delta \mathbf{X}_g(\delta I_\perp^P) = (q_1 + \delta q_1(\delta I_\perp^P), q_2 + \delta q_2(\delta I_\perp^P))$ according to Eqs. (13a), (13b).
3. Evaluate $\Delta\mu(\delta I_\perp^P)$ and $\Delta v_\parallel(\delta I_\perp^P, \delta \mathbf{X}_g)$, which are needed for the orbit tracing to the resonance point consistent with the corrector step, $\delta I_\perp^P$.
4. Effectuate the orbit tracing for finding the spatial location, $\mathbf{X}_{g,\Delta\tau_{res}} = (q_1 + \Delta q_1, q_2 + \Delta q_2)$, of the resonance.
5. Evaluate $\bar{b}_{0s,n}^P$ at the modified resonance position.
6. Calculate the corrector, i.e. the real step of the marker in phase space, $\Delta I_\perp$;
7. Move the marker to a spatial position of the updated orbit corresponding to $I_\perp(\tau_{n+1})$, i.e. $\Delta \mathbf{X}_g(\Delta I_\perp) = (q_1 + \Delta q_1(\Delta I_\perp), q_2 + \Delta q_2(\Delta I_\perp))$ according to Eqs. (13a), (13b).
8. Evaluate $\Delta\mu(\Delta I_\perp)$ and $\Delta v_\parallel(\Delta I_\perp, \Delta \mathbf{X}_g)$, which are needed at the start of the continued orbit tracing.
9. From this point the orbit following is resumed, without double counting the just treated resonance, until the intersection of the next resonance. In order to avoid double counting a resonance, one should in the case $\Delta\tau_{res} > 0$ inhibit detection of resonances for the just treated toroidal mode N for a time span of around $2\Delta\tau_{res}$.

This procedure is illustrated schematically in Fig. 4.

We have here outlined how the two-step Monte Carlo algorithm can be implemented. Of course there may be particular situations requiring special treatment (Monte Carlo codes have a habit of seeking out awkward cases). For instance, there may be markers for which the wave–particle interaction varies rapidly with their phase space position and the acceleration factor may be too large for them. Because the acceleration factor cannot be changed locally to adapt to such situations (it can only be changed once per calculated orbit) a special treatment is needed. In Appendix A an algorithm for dealing with such cases is discussed. There may also be other spacial cases that e.g. depend on the type of OFMC used requiring further modifications for individual markers.

4. Conclusions

A new two-step Monte Carlo algorithm accounting for resonant interaction between ions and RF waves in a toroidal plasmas has been presented. It is designed for orbit following Monte Carlo codes and addresses the fact that the resonance location is displaced by a resonant interaction. This displacement affects the expectation value of the Monte Carlo operator, and should be taken into account in detailed simulations of RF wave–particle interaction. There are two factors behind the displacement:

(i) the Doppler shift changes following a resonant interaction; (ii) the guiding centre position of a resonant particle evolves during a resonant interaction. The physics of the latter has been reviewed, and the key role played by the absorption of wave momentum for the evolution of the guiding centre position was demonstrated. However, for the Monte Carlo algorithm, the first factor has generally a significantly larger impact.

By using a suitably chosen set of invariants for the unperturbed motion of an ion, it was shown that the Monte Carlo algorithm can be reduced to updating just one invariant, $I_\perp$, for a given resonance point. From the update of this invariant, all the changes of the phase space variables of a particle can be derived. The fact that the Monte Carlo algorithm needs to act on only $I_\perp$ made it possible to develop the new two-step scheme where a predictor step, i.e. a fictitious intermediate step, is taken before the final updating of the position of a Monte Carlo marker in phase space. An advantage of this two-step scheme is that the quasi-linear diffusion coefficient needs to be evaluated in fewer phase space points than for the standard Euler–Maruyama scheme. This is important because it is computationally costly to find the spatial locations where the diffusion coefficient must be evaluated when the displacement of the resonance position is taken into account. Moreover, the new two-step algorithm was shown to have better strong convergence properties than the Euler–Maruyama scheme.

CRediT authorship contribution statement

T. Johnson: Writing – review & editing, Writing – original draft, Investigation, Formal analysis, Conceptualization. **L.-G. Eriksson:** Writing – review & editing, Writing – original draft, Methodology, Investigation, Formal analysis, Conceptualization.

Declaration of competing interest

The authors declare that they have no known competing financial interests or personal relationships that could have appeared to influence the work reported in this paper.

Data availability

No data was used for the research described in the article.

Acknowledgements

This work has been carried out within the framework of the EUROfusion Consortium, funded by the European Union via the Euratom Research and Training Programme (Grant Agreement No 101052200 - EUROfusion). Views and opinions expressed are however those of the author(s) only and do not necessarily reflect those of the European Union or the European Commission. Neither the European Union nor the European Commission can be held responsible for them.

Appendix A. Outline of steps leading to Eqs. (1)–(9)

The change in the parallel energy of an ion in a resonant interaction is obtained with the aid of Eq. (7b) as,

$$\begin{aligned} \Delta W_\parallel &= m v_\parallel \Delta v_\parallel = \Delta W - \Delta W_\perp \\ &= \Delta I_\perp - B\Delta\mu - \mu\Delta B = (1 - \frac{n\omega_c}{\omega})\Delta W - \mu\frac{\partial B}{\partial q_i}\Delta q_i \end{aligned} \tag{26}$$

and Eq. (10) follows directly from this expression. Next we consider the change in the toroidal angular momentum,

$$\Delta p_\phi = \frac{N}{\omega}\Delta I_\perp = m\left(\frac{\partial F}{\partial q_i}\frac{v_\parallel}{B} - \frac{F v_\parallel}{B^2}\frac{\partial B}{\partial q_i}\right)\Delta q_i + m\frac{F}{B}\Delta v_\parallel + Ze\frac{\partial \psi}{\partial q_i}\Delta q_i \tag{27}$$

Combining this equation with Eq. (10), observing that $\partial F/\partial q_i \Delta q_i = (\partial F/\partial\psi)\partial\psi/\partial q_i \Delta q_i$ and rearranging terms one arrive at Eqs. (9) and (11).

Appendix B. Numerical properties of the predictor–corrector two-step scheme

The predictor–corrector scheme presented in (22) has convergence properties similar to a Milstein scheme. In order to show this we Itô–Taylor expand $\bar{b}_{0s,n}^P$, ignoring terms of the order $\delta\tau$

$$\bar{b}_{0s,n}\left(I_\perp(\tau_n) + \delta\hat{I}_\perp^P(\tau_n)\right) \approx \bar{b}_{0s,n} + \bar{b}_{0s,n}\bar{b}'_{0s,n}\sqrt{N_{ACC}}W_1, \tag{28}$$

where the prime denotes a derivative with respect to $I_\perp$. Inserting this expansion and (21) into (22) we obtain, ignoring terms of order $dt^{3/2}$ or higher,

$$I_\perp(\tau_{n+1}) = I_\perp(\tau_n) + \frac{1}{2}\bar{b}_{0s,n}\bar{b}'_{0s,n}N_{ACC}(1 + W_1^2) + \bar{b}_{0s,n}\sqrt{N_{ACC}}W_1, \tag{29}$$

which is equivalent to the Milstein scheme [22]. Consequently, the two-step scheme has the same convergence properties as the Milstein scheme, i.e. both strong and weak convergence or order 1.

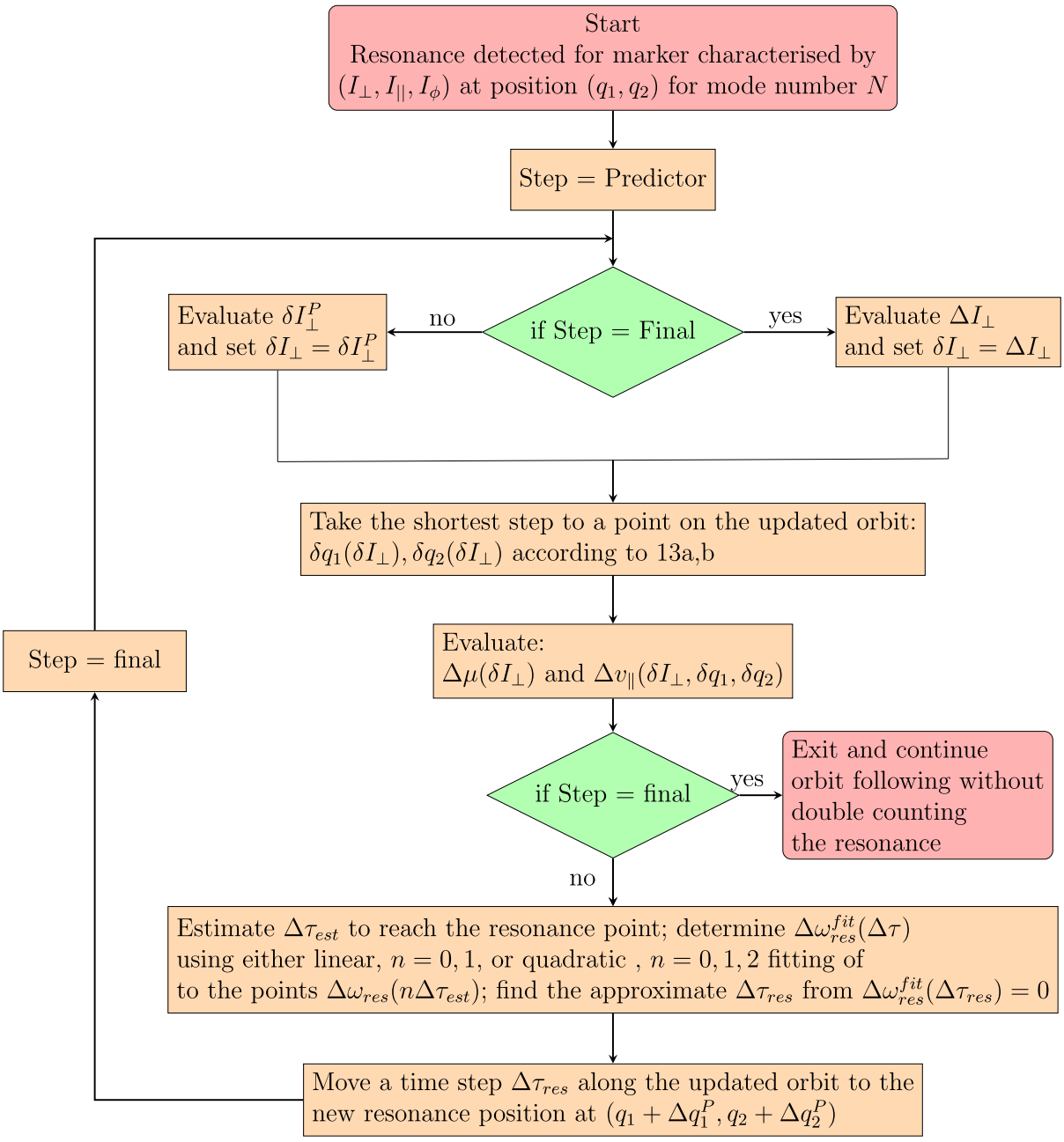

Fig. 4. Illustration of an implementation of the new two-step wave–particle interaction Monte Carlo operator.

Appendix C. Special treatment when N_{ACC} is detected to be too large

The acceleration factor, N_{ACC}, can of course only be changed once per calculated orbit revolution and while best effort is made to adjust it appropriately after each completed orbit it is inevitable that situations will occur where N_{ACC} is detected to be too large for a particular resonant interaction. There are basically three criteria for when N_{ACC} is too for an interaction:

- $\epsilon_D > \epsilon_{Dmax}$ where $\epsilon_D = \left|D_{0s}(I_\perp + \Delta I_\perp) - D_{0s}(I_\perp)\right| / D_{0s}(I_\perp)$, and ϵ_{Dmax} is a user defined maximum relative change that can be tolerated.
- The triplet of invariants $(I_\perp + \Delta I_\perp, I_\parallel, I_\phi)$ corresponds to an orbit that has no cyclotron resonances.
- The triplet of invariants $(I_\perp + \Delta I_\perp, I_\parallel, I_\phi)$ corresponds to a forbidden region in the invariant space (i.e. where the are no orbits, mostly when the update of $I_\perp$) results in a negative energy of magnetic momentum.

If any of these criteria are found to be fulfilled as a result of applying $\Delta I_\perp$, a corrective algorithm must be applied. It is important to note that in order to not bias the calculation, the total step in terms of W_1 (i.e. the one that went into to the evaluation of $\Delta I_\perp$) must remain the same. In practise this means inserting m sub time steps in the interval 0 to $\Delta\bar{t}$, i.e. 0 to 1, with constrained stochastic processes w_{Δ_j},

$$W_1 = \sum_{j=1,m} w_{\Delta_j}. \tag{30}$$

There are several ways of creating the constrained processes w_{Δ_j}. We have found it convenient to use a Brownian bridge, see e.g. [23]. Let us denote by B_i the evolution of the process up to sub-point i.

$$B_i = \sum_{j=1,i} w_{\Delta_j}. \tag{31}$$

Furthermore, assuming a uniform subdivision of the points the Brownian bridge algorithm yields the following expression for generating B_i from two points, k and l either side of it ($k < i$ and $l > i$),

$$B_i = \frac{B_k(l-i) + B_l(i-k)}{l-k} + Z_i\sqrt{\frac{(i-k)(l-i)}{l-k}}, \tag{32}$$

where Z_i is a normally distributed random number. There are a number of iterative sequences by which the B_i can be generated. In RFOF the interval is simply subdivided in successive midpoints, i.e. 2^m intervals for m subdivisions, and at each subdivision the above formula is used to obtain the B_i at a new midpoint from its neighbouring points as,

$$B_i = \frac{B_{i-1} + B_{i+1}}{2} + \frac{Z_i}{\sqrt{2}}. \tag{33}$$

The number of subdivisions, m, applied is discussed further down. From the B_i values, the w_{Δ_j} are then directly obtained. Armed with these the evaluation of two-step scheme is refined as,

$$I_{\perp}(\tau_{n+1}) = I_{\perp;m}, \tag{34a}$$

$$I_{\perp;i} = I_{\perp}(\tau_n) + \sum_{j=1}^{i} \Delta I_{\perp;j}, \tag{34b}$$

$$\delta I^P_{\perp;i} = \bar{b}_{0s;i}\sqrt{N_{ACC}}w_{\Delta_i}, \tag{34c}$$

$$\Delta I_{\perp;i} = \frac{1}{2}\bar{b}_{0s;i}\frac{\bar{b}^P_{0s;i} - \bar{b}_{0s;i}}{\delta I^P_{\perp;1}}N_{ACC} + \frac{1}{2}\left(\bar{b}^P_{0s;i} + \bar{b}_{0s;i}\right)\sqrt{N_{ACC}}w_{\Delta_i}, \tag{34d}$$

where $\bar{b}_{0s;i} = \bar{b}_{0s}(I_{\perp;i})$ and $\bar{b}^P_{0s;i} = \bar{b}_{0s}(I_{\perp;i} + \delta I^P_{\perp;i})$.

Because ϵ_{Di} for a sub-interval should scale roughly as $\sqrt{m}$, RFOF uses a first estimate for the number of subdivisions needed when the first condition above is fulfilled given by

$$m = \left\lceil 2\left[\frac{\epsilon_D}{\epsilon_{Dmax}}\right]^2\right\rceil, \tag{35}$$

where the outer bracket denotes the ceiling function. If this initial number of sub-divided intervals is found to be insufficient, successive additional subdivisions are made until ϵ_{Di} falls below ϵ_{Dmax} for all i. In the case of the updated invariants corresponding to a region in phase space with no orbits, successive subdivisions of the interval are carried out until the total change corresponds to a real orbit.

References

[1] F.S. Zaitsev, M.R. O'Brien, M. Cox, Phys. Fluids B 5 (1993) 509.
[2] Yu.V. Petrov, R.W. Harvay, Plasma Phys. Control. Fusion 58 (2016) 115001.
[3] R.J. Goldston, D.C. McCune, H.H. Towner, S.L. Davis, R.J. Hawryluk, G.L. Schmidt, J. Comput. Phys. 43 (1981) 61.
[4] M.A. Kovanen, W.G.F. Core, T. Hellsten, Nucl. Fusion 32 (1992) 787.
[5] J.A. Heikkinen, S.K. Sipilä, T.J.H. Pättikangas, Comput. Phys. Commun. 76 (1993) 215.
[6] V.S. Chan, S.C. Chiu, Y.A. Omelchenko, Phys. Plasmas 9 (2002) 501.
[7] L.-G. Eriksson, M. Schneider, Phys. Plasmas 12 (2005) 07254.
[8] T. Johnson, A. Salmi, G. Steinbrecher, L.-G. Eriksson, T. Hellsten, L.J. Höök, M. Schneider, ITM-TF Contributors AIP Conf. Proc. 1406 (2011) 373, http://dx.doi.org/10.1063/1.3664996.
[9] S. Sipilä, J. Varje, T. Johnson, R. Bilato, J. Galdón-Quiroga, A. Snicker, T. Kurki-Suonio, L. Sanchís, D. Silvagni, J. González-Martín, Nucl. Fusion 61 (2021) 086026.
[10] M. Schneider, et al., Nucl. Fusion 56 (2016) 112022.
[11] D. Van Eester, J. Plasma Phys. 60 (1998) 627.
[12] D. Van Eester, J. Plasma Phys. 65 (2001) 407.
[13] N. Mellet, et al., Comput. Phys. Comm. 12182 (2011) 570.
[14] B. Zaar, et al., Nucl. Fusion 64 (2024) 066017.
[15] A.N. Kaufman, Phys. Fluids 15 (1972) 1063.
[16] L.-G. Eriksson, P. Helander, Phys. Plasmas. 1 (1994) 308.
[17] A. Bécoulet, D.J. Gambier, A. Samain, Phys. Fluids B 3 (1991) 137.
[18] Y.O. Kazakov, et al., Nat. Phys. 13 (2017) 973.
[19] C.F.F. Karney, Phys. Fluids 22 (1979) 2188.
[20] N.J. Fisch, Phys. Plasmas 2 (1995) 2375.
[21] G. Steinbrecher, Priv. Commun. (2010).
[22] G.N. Milstein, Approximate integration of stochastic differential equations, Theory Probab. Appl. 19 (3) (1975) 557, http://dx.doi.org/10.1137/1119062.
[23] P. Glasserman, Monte Carlo Methods in Financial Engineering, Springer, 2004.